Micromagnetics of mesoscopic epitaxial (110) Fe elements with nanoshaped ends

J. Yu and U. Rüdiger
Department of Physics, New York University, 4 Washington Place, New York, New York 10003

L. Thomas and S. S. P. Parkin
IBM Research Division, Almaden Research Center, San Jose, California 95120

A. D. Kent[a)]
Department of Physics, New York University, 4 Washington Place, New York, New York 10003

The magnetization reversal and magnetic domain configurations of 0.5-μm-wide epitaxial (110) Fe particles with rectangular and needle-shaped ends and competing magnetic anisotropies have been investigated. Magnetic force microscopy imaging and longitudinal Kerr hysteresis loop measurements in conjunction with micromagnetic simulations have been used to elucidate the basic micromagnetic behavior. End shape is shown to be a determining factor for the nucleation of magnetization reversal and the resulting magnetic domain configurations.

I. INTRODUCTION

Nanostructured magnetic elements and multilayers are a topic of great interest with important applications to magnetic memories, high density recording media, and magnetic field sensors. For applications the ability to control the micromagnetic properties of magnetic particles such as the magnetic switching behavior, the coercivity, and long range interactions between individual particles, is essential. Epitaxial growth and microfabrication techniques enables the preparation of magnetic particles with interesting competitions between magnetocrystalline and shape anisotropy with unique and tractable properties. Here we present the initial results of such studies on submicron Fe elements which combine magnetic force microscopy (MFM), longitudinal Kerr hysteresis loop measurements (MOKE), and micromagnetic simulations to elucidate micromagnetic behavior.

II. FABRICATION AND CHARACTERIZATION

(110) oriented 50-nm-thick Fe films are grown on *a*-axis (11-20) sapphire substrate using ultrahigh vacuum (UHV) e-beam evaporation techniques. The details of the deposition process are described in Ref. 1. An anisotropic in-plane strain in these films induces a strong in-plane uniaxial magnetic anisotropy, with the easy axis along the [001] direction.[2] For an unpatterned (110) Fe film the hysteresis loop with an applied magnetic field parallel to the [1-10] is consistent with two and four fold components of the magnetic anisotropy. This loop has been fitted for a 50-nm-thick (110) Fe film using the in-plane anisotropy energy

$$E=(K_1+K_u)\sin^2\Theta-3K_1/4\sin^4\Theta, \quad (1)$$

where K_1 is the cubic anisotropy constant, K_u is the uniaxial anisotropy constant, and Θ is the angle between the magnetization and the [001] easy magnetic axis. From this fit the cubic and the uniaxial anisotropy constants have been determined to be $K_1=6.3\times10^5$ and $K_u=3.0\times10^5$ erg/cm^3.

These (110) Fe films have been patterned into particle arrays with a variety of shapes and sizes, using electron beam lithography and ion milling. The magnetic properties and the magnetization reversal process were studied via MOKE and MFM.[3] Here we report results on 0.5-μm-wide particles. Figure 1 shows scanning electron microscopy (SEM) images of these particles with rectangular and needle-shaped ends. The rectangular particles have a length-to-width ratio of 3:1, while the other type have two additional needle-like ends. All the particles are separated by four times their width and three times their length, so that dipolar interaction between neighboring particles are negligible. The long axis of the particle is oriented parallel to the in-plane Fe [1-10] direction, hence perpendicular to the in-plane magnetocrystalline easy axis.

III. RESULTS

Figure 2 shows the hysteresis loops of rectangular and needle-like end particles in longitudinal and transverse geometry. *H* longitudinal refers to the applied magnetic field parallel to the long axis of the particle while *H* transverse refers to the field perpendicular to the long axis (i.e.,

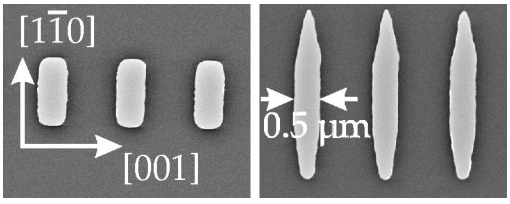

FIG. 1. SEM images of rectangular and needle-shaped (110) Fe particles. The [001] easy magnetocrystalline axis is oriented perpendicular to the long wire axis.

[a)]Electronic mail: adkl@is.nyu.edu

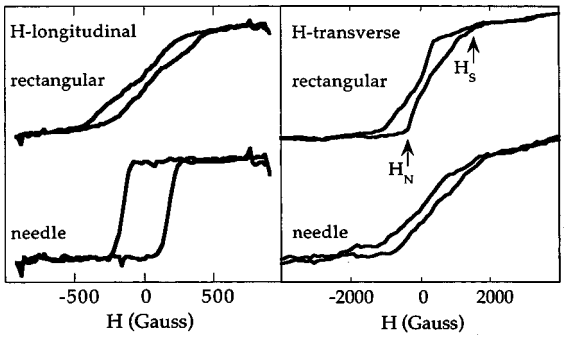

FIG. 2. Longitudinal MOKE hysteresis loop measurements on rectangular and needle-shaped (110) Fe particles with the applied magnetic field perpendicular (H transverse) and parallel (H longitudinal) to the long axis of the particles.

$H \| [001]$). In the transverse case the hysteresis loops of rectangular and needle-like end particles both exhibit almost a fully demagnetized state at $H=0$. For rectangular particles the saturation field H_S and the nucleation field H_N are determined to be $H_S=1700$ and $H_N=400$ G. For needle-like particles H_S is 2000 G and H_N is 750 G. The particles with needle-shaped ends have higher nucleation and saturation fields.

In the longitudinal case the rectangular particles show a fully demagnetized state at zero applied field, a nucleation field of only $H_N=250$ G, and the magnetic saturation occurs at only $H_S=450$ G. In contrast, the needle-like end particles show a square hysteresis loop with full remanence and a saturation field of only $H_S=250$ G.

MFM imaging of these Fe particles has been done in order to understand the influence of the particles shape and the magnetic history on the magnetic domain configurations at $H=0$. The CoCr coated MFM tips used are vertically magnetized highlighting the magnetic poles at the boundaries of particles and the out-of-plane magnetization component of the domain walls.

In Fig. 3, the rectangular particle shows a multidomain configuration where the size of the domains depends on the magnetic history such as the previous saturation direction. The arrows in Fig. 3(a) indicate the in-plane magnetization direction of the stripe domains with the magnetization parallel or antiparallel to the easy magnetic axis and the flux closure domains where the magnetization is directed perpendicular to the easy axis. These MFM images of the

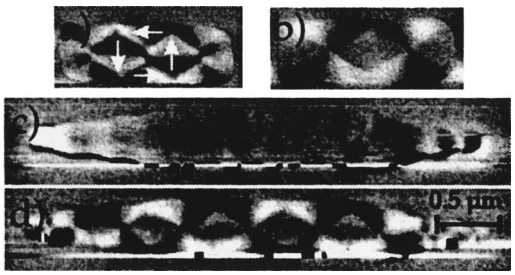

FIG. 3. MFM images at $H=0$ on rectangular and needle-shaped (110) Fe particles after (a) and (c) longitudinal saturation and after (b) and (d) transverse magnetic saturation.

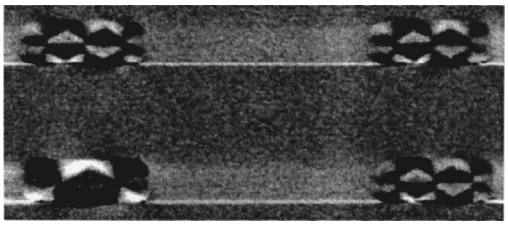

FIG. 4. MFM image at $H=0$ of an array of rectangular (110) Fe particles after longitudinal magnetic saturation.

demagnetized state at $H=0$ are consistent with the small remanence seen in MOKE hysteresis loops. The most striking feature is the smaller stripe domain width after longitudinal saturation in comparison with the domain width after transverse saturation. The magnetic domain configurations shown in Figs. 3(a) and 3(b) are the median domain configurations of a large number of particles in an array of nominally identical particles. The MFM image in Fig. 4 shows that rectangular particles can have different domain configurations after longitudinal saturation.

The needle-like particle [see Fig. 3(c)] shows a fully saturated state after longitudinal saturation which is in agreement with the corresponding MOKE hysteresis loop measurement (Fig. 2). In contrast, after transverse saturation the observed domain pattern corresponds to a fully demagnetized state.

IV. DISCUSSION

The interplay of exchange, shape, and magnetocrystalline anisotropy energies determines the micromagnetic structure and magnetization reversal process. With decreasing particle size, the demagnetizing field arising from the magnetic charges formed at particle edges becomes important. It introduces a shape anisotropy with easy axis parallel to the long axis of the particle, which is perpendicular to the magnetocrystalline easy axis.

It is well known that for magnetic systems with an easy magnetocrystalline axis perpendicular to the long axis of the structure a stripe domain configuration minimizes the free energy.[4] Due to the small ratio of magnetocrystalline anisotropy to demagnetization energy $Q=(K_1+K_u)/2\pi M^2 \approx 0.05$, stripe domains in conjunction with flux closure domains at $H=0$ are energetically favored. Such domain configurations have been observed on wires,[1,5] rectangular particles, and partly needle-shaped particles.

However, nucleation barriers must be overcome to form stripe domain states. In the transverse case, both for rectangular and needle-shaped particles, domains nucleate near the particle ends.[3] The demagnetizing field at the end of needle-shaped particles is much stronger than that at the corners of the rectangular particles and, therefore, leads to higher nucleation and saturation fields for needle-like end particles. After nucleation of magnetic domains at the ends of the particle, the domains move towards the particle center, thus forming a flux closure multidomain state at $H=0$.

For the longitudinal case both the shape anisotropy and Zeeman energy favor a magnetization parallel to the applied

field. Therefore, the nucleation field is smaller compared to the transverse case. When domains nucleate, the reduced nucleation field gives rise to a smaller volume of flux closure domains (due to the reduced Zeeman energy) and thus a greater number of domains in comparison with the transverse geometry. On further reduction of the applied field no new domains are nucleated, so the stripe domain size is smaller after longitudinal saturation in rectangular particles.[5] For the needle-like end particles the shape anisotropy overwhelms the magnetocrystalline anisotropy and suppresses the nucleation of domains completely, resulting in a fully saturated state at $H=0$.

There are clearly differences among nominally identical particles in an array such as roughness of the edges, shape of the corners, and locations of imperfections. All of these influence the amplitude of the nucleation field, as well as details of the magnetization reversal, which in turn influence the domain size at $H=0$. The MFM image of the magnetic domain configurations of four identical rectangular (110) Fe particles shown in Fig. 4 were performed after longitudinal saturation. Three particles contain two stripe domains whereas one exhibits a domain configuration with only one stripe domain. This MFM image has been repeated many times each after longitudinal saturation but no change of the individually domain configuration of a given particle has been observed. This suggests that the exact domain configuration of an individual particle is more strongly influenced by the specific particle properties than the stochastic nature of the magnetization reversal.

V. MICROMAGNETIC SIMULATIONS

The magnetic domain patterns of a 50-nm-thick rectangular Fe particle with lateral dimensions of 1500 nm by 500 nm has been computed at zero magnetic field with the Landau–Lifschitz–Gilber (LLG) micromagnetics simulator.[6] The corners have been rounded to reproduce the imperfections of the actual shape of the particles. The equilibrium magnetization was found by solving the LLG equation.[7] In this equation, the effective field acting on the spins is determined from the total energy of the system, which incorporates the effect of exchange, magnetocrystalline anisotropy, magnetostatic, and Zeeman terms. The continuous magnetization distribution was approximated by a discrete cubic mesh, with a cell volume of 1000 nm^3. Tests performed using a finer grid have shown similar results.

Figure 5 shows the simulated magnetic domain configuration at zero magnetic field starting from a saturated state in (a) transverse and (b) longitudinal direction assuming $K_1=6.3\times10^5$ and $K_u=3\times10^5$ erg/cm^3. Note that this procedure corresponds to a fast removal of the saturation field and is not the same as in the experiment. The arrows indicate the in-plane magnetization direction of the stripe and flux closure domains. In comparison to the experimentally observed magnetic domain pattern shown in Figs. 3(a) and 3(b) the presence of stripe and flux closure domains is reproduced but

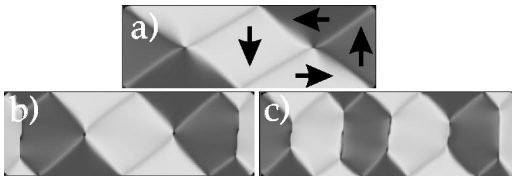

FIG. 5. Calculated magnetic domain pattern at $H=0$ after (a) transverse and (b) longitudinal saturation. In comparison to (b) in (c) the corner geometry slightly changed.

in the longitudinal case the width of the stripe domains differs from the experimental data. The difference between the experimental and calculated magnetic domain pattern could originate from both a deviation in the uniaxial anisotropy constant and the real geometry as well as crystalline imperfections of the Fe particles, i.e., rounded edges and corners due to the fabrication process, which have a strong impact on the nucleation process of magnetic domains just below the saturation field. The calculated equilibrium domain patterns have been found to depend strongly on imperfections added to the perfect square shape. Figure 5(c) shows the magnetic domain pattern after longitudinal saturation with slightly different corner geometry as used for the calculation of Fig. 5(b) which leads to significant change of the stripe domain size.

VI. SUMMARY

In summary, the influence of the end shape and the magnetic history on the magnetic domain configuration of epitaxial (110) Fe particles has been studied. Nucleation of the magnetization reversal, which occurs at the particle ends, can be changed by varying particle end shape. However, less controllable properties like crystalline imperfections, rounded edges and corners, and edge roughness also play an important role and have been shown to lead to different magnetic domain configurations in an array of nominally identical particles.

ACKNOWLEDGMENTS

This research was supported by DARPA-ONR, Grant No. N00014-96-1-1207. Microstructures were prepared at the CNF, Project No. 588-96.

[1] A. D. Kent, U. Rüdiger, J. Yu, S. Zhang, P. M. Levy, and S. S. P. Parkin, IEEE Trans. Magn. **34**, 900 (1998).
[2] B. M. Clemens, R. Osgood, A. P. Payne, B. M. Lairson, S. Brennan, R. L. White, and W. D. Nix, J. Magn. Magn. Mater. **121**, 37 (1993).
[3] J. Yu, U. Rüdiger, A. D. Kent, L. Thomas, and S. S. P. Parkin, Phys. Rev. B (submitted).
[4] C. Kittel, Phys. Rev. **70**, 965 (1946).
[5] U. Rüdiger, J. Yu, S. S. P. Parkin, and A. D. Kent, Appl. Phys. Lett. **73**, 1298 (1998).
[6] M. R. Scheinfein *et al.*, Phys. Rev. B **43**, 3395 (1991); www.dancris.com\~11g.
[7] A. Aharoni, *Introduction to the Theory of Ferromagnetism* (Clarendon, Oxford, 1996).